

# CREEP FORCES IN SIMULATIONS OF TRACTION VEHICLES RUNNING ON ADHESION LIMIT

Oldrich Polach

Bombardier Transportation, CH-8401 Winterthur  
SWITZERLAND

[oldrich.polach@ch.transport.bombardier.com](mailto:oldrich.polach@ch.transport.bombardier.com)

## Abstract

A necessary condition for complex simulations of vehicle system dynamics including drive dynamics and traction control when running on adhesion limit, is an advanced creep force modelling taking large longitudinal creep into account. A method presented in the paper allows to simulate various real wheel-rail contact conditions using one parameter set identified from measurements. Influence of vehicle speed, longitudinal, lateral and spin creep and shape of the contact ellipse is also considered. The method was validated by comparisons with measurements as presented in application examples.

## INTRODUCTION

High adhesion utilisation and sophisticated vehicle dynamics design of modern locomotives and traction vehicles demands complex simulations which simultaneously take into consideration the mechanical, electrotechnical and control system fields.

In computer simulations, different methods are used to calculate tangential creep forces between wheel and rail:

- for general vehicle dynamic calculations, without or with small tractive forces
- for analysis of traction chain dynamics and traction control with high tractive forces.

In vehicle dynamics, small creep values (microslip) are of main importance. Longitudinal and lateral creep as well as spin should be taken into account. The friction coefficient is assumed to be constant. The difference between dry and wet conditions is usually expressed only with the value of the friction coefficient.

In traction chain dynamics usually only the longitudinal direction is taken into account. There is a maximum of creepforce-creep-function and a decreasing section behind this maximum. The initial slope and the form the functions for wet, dry or polluted conditions are different.

For a complex simulation of dynamic behaviour of a locomotive in connection with drive dynamics and

traction control, the different creep force models described above have to be made into one model. A possible method is described in this paper and its application illustrated in examples.

## A CREEP FORCE MODEL FOR SIMULATIONS OF TRACTION VEHICLES RUNNING ON ADHESION LIMIT

A possible explanation of the decreasing section of creepforce-creep-function for large longitudinal creep is the decrease of friction coefficient with increasing slip velocity due to increasing temperature in the contact area [1, 2, 3, 4, 5]. Another explanation - different friction coefficients in the area of adhesion and area of slip (static and kinematic friction coefficient) – does not seem to sufficiently influence the shape of the creep force curve [5].

The assumption of friction coefficient decreasing with increasing temperature usually leads to good agreement between theory and measurements for dry and clean contact conditions. The agreement is worse for contaminated surfaces. For wet conditions, an interfacial layer of liquid should be considered. In spite of several published theories considering a layer of liquid or moisture, there is no simple model existing to simulate dry as well as wet conditions in contact of wheel and rail in computer simulations.

The method described in this paper allows to simulate creep forces according to measurements for various contact conditions – dry, wet, polluted etc. It is based on a fast method for calculation of wheel-rail forces developed by the author and largely tested and used in various three-dimensional multi-body simulation tools. The original method is presented briefly in the next chapter. Then, a possible modelling of friction coefficient decreasing with increasing slip velocity together with the reduction of initial slope of creep force curve will be shown and the limitations of this model explained. Later, an extension by different reduction factors in the area of adhesion and area of slip will be presented and the contact model parameters identified by comparisons with measurements. The extended method allows to model the creep forces in

multi-body simulations for various contact conditions in good agreement with measurements.

### *A fast method for calculation of creep forces in multi-body simulation*

The method developed by the author for calculation of creep forces in multi-body simulations [6, 7] is based on a theoretical model for longitudinal and lateral creep assuming a coefficient characterising the contact shear stiffness.

The contact area is assumed elliptical with half-axes  $a$ ,  $b$  and normal stress distribution according to Hertz. The maximum value of tangential stress  $\tau$  at any arbitrary point is

$$\tau_{\max} = \mu \cdot \sigma \quad (1)$$

where

$\mu$  - coefficient of friction,  
 $\sigma$  - normal stress.

The solution leads to the resultant tangential force (without spin) as

$$F = \frac{2 \cdot \mu \cdot Q}{\pi} \left( \frac{\varepsilon}{1 + \varepsilon^2} + \arctan \varepsilon \right) \quad (2)$$

where

$Q$  - wheel load  
 $\varepsilon$  - gradient of the tangential stress in the area of adhesion

$$\varepsilon = \frac{2}{3} \frac{C \cdot \pi \cdot a^2 \cdot b}{Q \cdot \mu} s \quad (3)$$

where

$C$  - proportionality coefficient characterising the contact shear stiffness [N/m<sup>3</sup>]  
 $a, b$  - half-axes of the contact ellipse  
 $s$  - creep

$$s = \sqrt{s_x^2 + s_y^2} \quad (4)$$

$$s_i = \frac{w_i}{V} \quad i = x, y \quad (5)$$

where

$s_x, s_y$  - creep in longitudinal ( $x$ ) and lateral ( $y$ ) directions  
 $w_x, w_y$  - creep (slip) velocity in longitudinal ( $x$ ) and lateral ( $y$ ) directions  
 $V$  - vehicle speed.

The forces  $F_x, F_y$  and the adhesion coefficients  $f_x, f_y$  in longitudinal and lateral directions are

$$F_i = F \frac{s_i}{s} \quad i = x, y \quad (6)$$

$$f_i = \frac{F_i}{Q} \quad i = x, y \quad (7)$$

Based on Kalker's results, the influence of spin was introduced as described in [6, 7], so that the method can be used for general conditions of longitudinal, lateral and spin creep. A detailed description and computer code can be found in [7].

Comparisons with other methods used in computer simulations give very good results. Deriving the contact shear stiffness coefficient  $C$  from Kalker's linear theory [8], the method is used as a simple and fast alternative instead of the FASTSIM computer code [9] or other methods or pre-calculated tables. The method is faster than FASTSIM and approximately as fast as the method developed by Shen-Hedrick-Elkins [10], but the results are closer to FASTSIM than other methods. The method was implemented into simulation tools ADAMS/Rail, SIMPACK, GENSY and used in other tools as user routine as well.

### *Friction coefficient dependent on slip velocity*

A creep-force law with a marked adhesion optimum can be modelled using the friction coefficient decreasing with increasing slip (creep) velocity between wheel and rail [11, 12]. The dependence of friction on the slip velocity was observed by various authors and is described e. g. in [13]. The variable friction coefficient can be expressed by the following equation

$$\mu = \mu_0 \cdot \left[ (1 - A) \cdot e^{-B \cdot w} + A \right] \quad (8)$$

where

$\mu_0$  - maximum friction coefficient  
 $w$  - magnitude of the slip (creep) velocity vector [m/s]  
 $B$  - coefficient of exponential friction decrease [s/m]  
 $A$  - ratio of limit friction coefficient  $\mu_\infty$  at infinity slip velocity to maximum friction coefficient  $\mu_0$

$$A = \frac{\mu_\infty}{\mu_0} \quad (9)$$

In recent years, theoretical studies have been published explaining the decreasing section of creep-force function under the influence of temperature in the contact area [1, 2, 3, 4]. With increasing creep, the temperature in the contact area increases and the coefficient of friction decreases.

In addition, the reduction  $k < 1$  of the initial slope of creep force curve explained in [4, 14] through the influence of the surface roughness and in [15, 16] by effect of contamination can be used. Using these assumptions, a good agreement between theory and measurements can be found in some cases for dry or slightly contaminated conditions. For wet or polluted

conditions however, a layer of liquid or contaminants should be considered which have not been included in the above theory. A large longitudinal slip between wheel and rail occurs for the adhesion limit, in particular for the maximum transmissible tractive forces.

Using the theory of friction coefficient decreasing with increasing slip by the influence of temperature for the case of wet or polluted contact conditions, the only way to achieve the adhesion optimum at large creep values is a significant reduction of the coefficients of Kalker's linear theory ( $k < 0.1$ ), see *figure 1*. But the measurements of the initial slope of creepforce-creep-function do not show such low values. Typical values of the reduction factor for real wheel-rail contact conditions are 0.2 – 0.5 for wet rails and 0.6 – 0.85 for dry rails. It means that using the temperature influence only does not allow to simulate the contact of wheel and rail in complex dynamics simulations when transmitting the limiting tractive forces under unfavourable adhesion conditions.

An extension of the fast method for calculation of creep forces presented in the next chapter allows to adapt the creep-force model for various conditions of wheel-rail contact according to measurements.

### An extended creep force model for large creep applications

The simplified modelling of the influence of real contact conditions with a layer of liquid or moisture can be explained as a combination of dry and wet friction. For small creep values, the area of adhesion extends to the greater part of the contact area. The conditions are similar to dry friction. For large creep values, there is slip in the main part of the contact area. The layer of water or pollution influences the resultant force. The stiffness of the anisotropic surface layer (called by Kalker "Steifheit der anisotropen Oberflächenschicht" in [15]) decreases and, as a result of this, the creepforce-creep-function reduces its gradient significantly.

To model these conditions, different reduction factors  $k_A$  in the area of adhesion and  $k_S$  in the area of slip are used. This is easily possible using the proposed method because there are two terms in the equation (2); the first one related to the area of adhesion and the second to the area of slip. The equation (2) has then the form

$$F = \frac{2 \cdot \mu \cdot Q}{\pi} \left( \frac{k_A \cdot \varepsilon}{1 + (k_A \cdot \varepsilon)^2} + \arctan(k_S \cdot \varepsilon) \right) \quad (10)$$

where  $k_A$  - reduction factor in the area of adhesion  
 $k_S$  - reduction factor in the area of slip

with

$$k_S \leq k_A \leq 1 \quad (11)$$

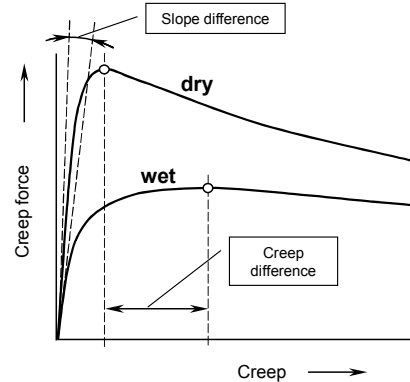


figure 1 Relation between the initial slope of creep force curve and its maximum (dry and wet)

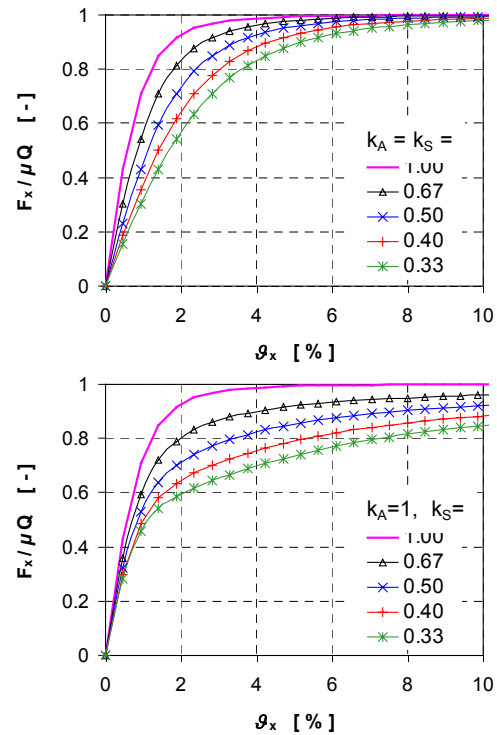


figure 2 Reduction of Kalker's coefficients with one factor (top) and using two different reduction factors (bottom)

The gradient of the creepforce-creep-function at the origin of the coordinates corresponds to the reduction of Kalker's coefficient

$$k = \frac{k_A + k_S}{2} \quad (12)$$

Using different reduction factors in the area of adhesion and in the area of slip for a constant friction coefficient there is hardly any reduction of the function gradient at small creepages but a significant reduction of the gradient near saturation, see *figure 2*.

The proposed extension by two reduction factors together with the friction coefficient decreasing with increasing slip (creep) velocity allows to reach the forms of creep force curves more similar to the measurements for various conditions.

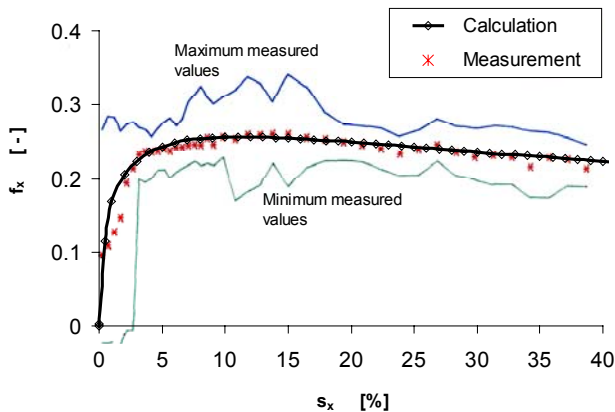


*figure 3* Model of creep forces based on the measurements with the Bombardier locomotive SBB 460 (wet,  $V = 40$  km/h)

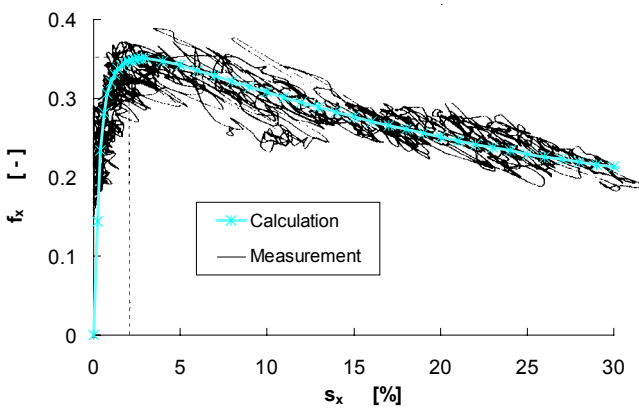


*figure 4* Model of creep forces based on the measurements with the Siemens locomotive S 252 (dry,  $V = 30$  km/h)

#### Parameter identification from measurements

The parameters of reduction factors  $k_A$ ,  $k_S$  and of the friction coefficient function have to be found by comparison of measured and computed creepforce-creep-functions for longitudinal direction.

Using the proposed method, the following measurements were modelled:

- Measurements with the Bombardier locomotive SBB 460 [17] on artificially watered rails, see *figure 3*
- Measurements with the Bombardier test locomotive 12X (DB 128) [18] on artificially watered rails with speeds of 20 and 60 km/h
- Measurements on GM locomotives SD 45X in the U.S.A. [19], on wet and dry rails with speeds between 16-32 km/h
- Measurements with the Siemens locomotive DB 127 Europrinter (according to [20]), dry rails, speed 32 km/h
- Measurements with the Siemens locomotive S 252 (according to [21] a typical shape of creep force curve on dry rails) – see *figure 4*

The parameters of creep force models shows *table 1*.

The models were tested for various speeds and for a range of longitudinal creepages from very small to large values. Even in this large range the results are plausible and the model is not limited to one speed or to a small creep range. In this way, the influence of speed on the form and maximum of creep force curves is expressed with only one parameter set, see *figure 5*.

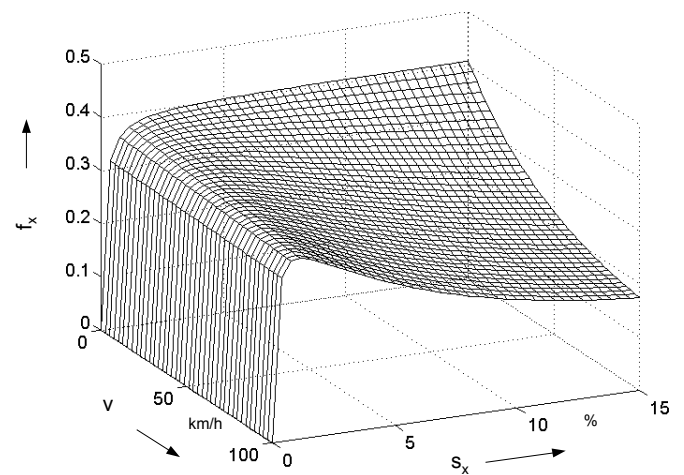


*figure 5* Influence of vehicle speed on the form of creepforce-creep-functions for longitudinal direction (model parameters according to measurement in *figure 4*)

Besides this, the influence of longitudinal, lateral and spin creep as well as the shape of the contact ellipse is also taken into account, *figure 6* (for other examples see [12]). Of course, a change of surface conditions (dry, wet etc.) as well as other effects, e. g. the cleaning effect due to large longitudinal creep (so-called rail conditioning), will cause a change of model parameters.

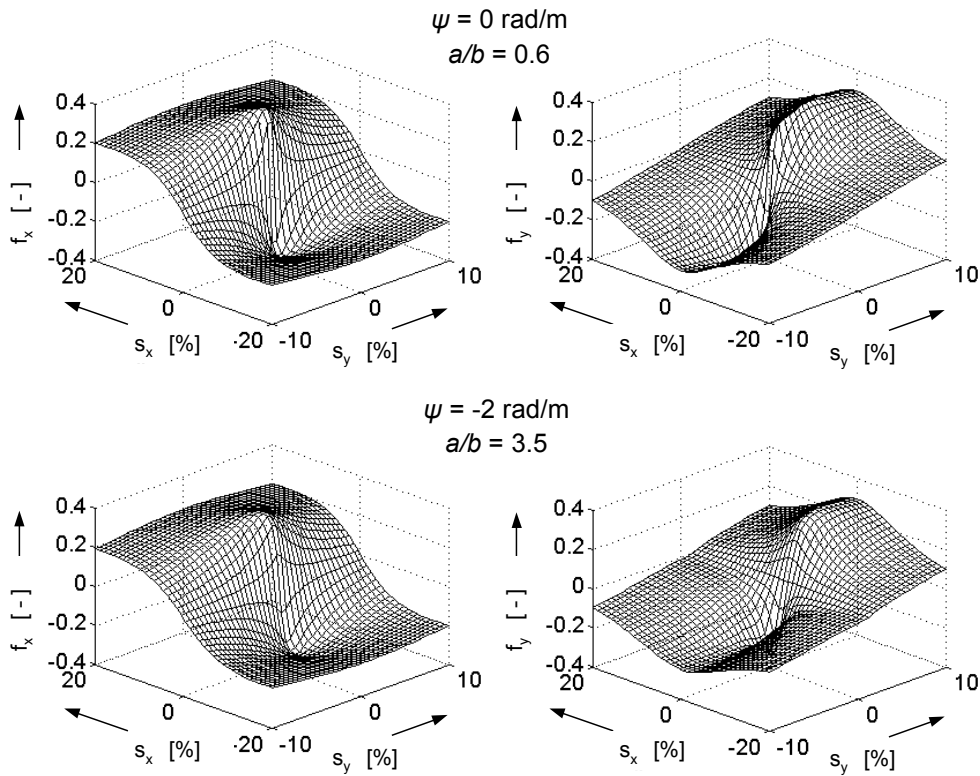


figure 6 Creep force coefficients according to the proposed extended method in function of longitudinal ( $s_x$ ), lateral ( $s_y$ ) and spin ( $\psi$ ) creepages as well as of the form of the contact area ( $a/b$ ); model parameters according to measurement in figure 4

## MODEL VALIDATION BY COMPARISON OF SIMULATIONS AND MEASUREMENTS

### *Influence of tractive force on the steering of a self-steering bogie*

In order to test the possibility of simulating the dynamic change of traction torque, a test case used during the adhesion test [17] of the four axle SBB 460 locomotive of the Swiss Federal Railways was simulated. The locomotive design combines very good curving performance with high maximum speed due to the coupling of wheelsets, realised by a mechanism with a torsional shaft assembled to the bogie frame. The locomotive model in simulation tool ADAMS/Rail consists of 51 rigid bodies and contains 266 degrees of freedom.

In the course of curving simulation, the traction torque was increased from zero to the adhesion limit, in a similar way as during the adhesion test measurements. In this manner, a run on the unstable (decreasing) section of creep force curve was simulated [22].

With increasing tractive effort, the wheelset steering ability decreases. Simultaneously, the first

wheelset of the bogie moves to the inner rail. The calculated steering angle as a function of tractive force in the steering linkages is compared with measurement in figure 7. The comparison confirms a good agreement in the tendency although the real track irregularity is not known in detail.

### *Co-simulation of vehicle dynamics and traction control*

In following application examples, the creep force model described above was used in a co-simulation of vehicle dynamics and traction control under bad adhesion conditions. The vehicle model is represented by the locomotive 12X of Bombardier Transportation (in service at the German Railways as DB 127) modelled in the simulation tool SIMPACK. The controller was modelled in computer code MATLAB-SIMULINK. During co-simulation, both programs are running in parallel exchanging few channels only, see [18, 23] for details.

As an application example, the traction control reaction following a sudden worsening of adhesion conditions was simulated and results published in [18, 23]. The assumed wheel-rail friction coefficient was suddenly reduced after approx. 30 m distance. Besides of this, small stochastic oscillations were superimposed. After the sudden reduction of friction coefficient, the

| Vehicle                        | SBB 460  | 12X            | SD 45X       | SD 45X       | DB 127   | S 252    |      |
|--------------------------------|----------|----------------|--------------|--------------|----------|----------|------|
| Wheel-rail conditions          | wet      | wet            | wet          | dry          | dry      | dry      |      |
| Speed                          | 40 km/h  | 20 and 60 km/h | 16 - 32 km/h | 16 - 32 km/h | 36 km/h  | 30 km/h  |      |
| Reference (measurement)        | [17]     | [18]           | [19]         | [19]         | [20]     | [21]     |      |
| Comparison model - measurement | figure 3 | see [18]       | see [12]     | see [12]     | see [12] | figure 4 |      |
| Modelparameter                 | Unit     |                |              |              |          |          |      |
| $k_A$                          | -        | 0.16           | 0.65         | 0.29         | 0.68     | 0.72     | 1    |
| $k_S$                          | -        | 0.07           | 0.26         | 0.07         | 0.14     | 0.36     | 0.6  |
| $\mu_0$                        | -        | 0.31           | 0.28         | 0.3          | 0.4      | 0.36     | 0.41 |
| $A$                            | -        | 0.5            | 0.4          | 0.38         | 0.44     | 0.38     | 0.36 |
| $B$                            | s/m      | 0.16           | 0.4          | 0.18         | 0.6      | 0.7      | 0.55 |
| $k$                            | -        | 0.115          | 0.455        | 0.18         | 0.41     | 0.54     | 0.8  |

table 1 Parameters of extended creep force model identified from measurements

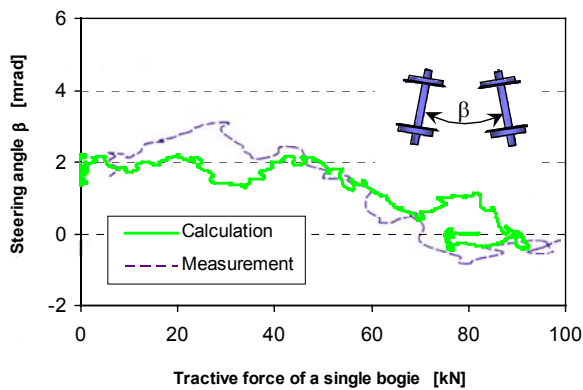


figure 7 Comparison of the measured and calculated steering angle between wheelsets as function of tractive effort of a single bogie

creep first increases, but the controller stabilises the working point at a new adhesion optimum with low creepage after a short transition period.

Another co-simulation study shows a starting and acceleration of locomotive hauling a train on a curved sloping track [18, 23]. Figure 8 presents a comparison of measurement and simulation of longitudinal forces in wheelset linkages. The observed forces on the straight track and on the left and right curves are very close in measurement and simulation. The comparison validates the proposed method as suitable for computer simulation of traction vehicles running on adhesion limit.

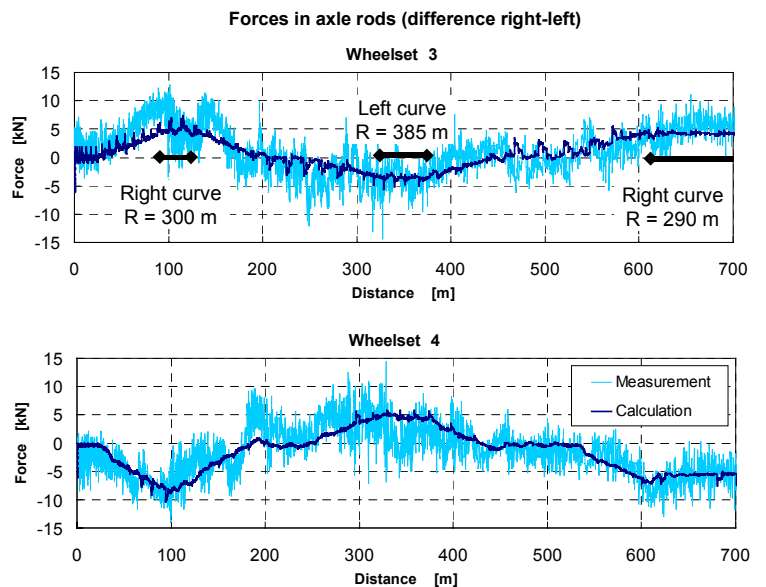


figure 8 Comparison of measured (non-filtered) and calculated forces in the longitudinal axle guidance during a start and acceleration of the test locomotive 12X on a curved track

## CONCLUSION

The proposed method for calculation of wheel-rail forces enables computer simulations of complex vehicle system dynamics including running and traction dynamics for large traction creep when running on adhesion limit. It allows to simulate various wheel-rail contact conditions based on the measured creepforce-creep-curves using one parameter set for various speeds.



The method was used in complex simulations of adhesion tests and traction control during an acceleration on curved lines and validated by comparisons with measurements.

## References

1. RICK, F: **Zur Erfassung der Geschwindigkeitsabhängigkeit des Kraftschlussbeiwertes eines hochbelasteten Rad-Schiene-Kontaktes**, Thesis, Technical University Clausthal, Germany, 1998
2. SCHWARZE, H: **Geschwindigkeitsabhängiger Kraftschluss hochbelasteter Rad-Schiene-Kontakte**, *Elektrische Bahnen*, 99(2001), No. 5, pp. 203-218
3. HOU, K & KALOUSEK, J: **Thermal effect on adhesion in wheel/rail interface**, *Proc. of the 5th International Conference „Contact Mechanics and Wear of Rail Wheel Systems*, Tokyo, Japan, 25-28 July 2000, pp. 239-244
4. ERTZ, M & BUCHER, F: **Improved creep force model for wheel/rail contact considering roughness and temperature**, *Proc. of the 17th IAVSD Symposium, Lyngby, Denmark, August 20-24, 2001, Vehicle System Dynamics Supplement*, 37 (2002), pp. 314-325
5. NIELSEN, J B & THEILER, A: **Tangential contact problem with friction coefficients depending on sliding velocity**, *Proc. of the 2nd Mini Conference on Contact Mechanics and Wear of Rail/Wheel Systems*, Budapest, July 29-31, 1996, pp. 44-51
6. POLACH, O: **Solution of wheel-rail contact forces suitable for calculation of rail vehicle dynamics**, *Proc. of the 2nd Int. Conference on Railway Bogies*, Budapest, Sept. 14-16, 1992, pp. 10-17
7. POLACH, O: **A Fast Wheel-Rail Forces Calculation Computer Code**, *Proc. of the 16th IAVSD Symposium, Pretoria, August 1999, Vehicle System Dynamics Supplement*, 33 (1999), pp. 728-739
8. KALKER, J J: **On the rolling contact of two elastic bodies in the presence of dry friction**, Thesis, Delft, 1967
9. KALKER, J J: **A fast algorithm for the simplified theory of rolling contact**, *Vehicle System Dynamics*, 11 (1982), pp. 1-13
10. SHEN, Z Y, HEDRICK, J K & ELKINS, J A: **A comparison of alternative creep force models for rail vehicle dynamic analysis**, *Proc. of the 8th IAVSD-Symposium*, Cambridge, MA, August 15-19, 1983, pp. 591-605
11. HÄSE, P & MENTH, S: **Kraftschluss bei Triebfahrzeugen – Modellbildung und Verifikation an Messdaten**, *Elektrische Bahnen*, 94 (1996), H. 5, S. 125-134
12. POLACH, O: **Rad-Schiene-Modelle in der Simulation der Fahrzeug- und Antriebsdynamik**, *Elektrische Bahnen*, 99(2001), No. 5, pp. 219-230
13. RABINOWICZ, E: **Friction and wear of materials**, John Wiley and Sons, New York, 1965
14. BUCHER, F, KNOTHE, K & THEILER, A: **Normal and tangential contact problem of surfaces with measured roughness**, *Proc. of the 5th International Conference „Contact Mechanics and Wear of Rail Wheel Systems”*, Tokyo, Japan, 25-28 July 2000, pp. 96-103
15. KALKER, J J: **Über die Mechanik des Kontaktes zwischen Rad und Schiene**, *ZEV-Glaser Annalen*, 102 (1978), pp. 214-218
16. HARRISON, H, MCCANNEY, T & COTTER, J: **Recent developments in COF measurements at the rail/wheel interface**, *Proc. of the 5th International Conference „Contact Mechanics and Wear of Rail Wheel Systems”*, Tokyo, Japan, 25-28 July 2000, pp. 30-35
17. POLACH, O: **SBB 460 Adhäsionsversuche**, Techn. Report No. 414, SLM Winterthur, 1992
18. POLACH, O: **Optimierung moderner Lok-Drehgestelle durch fahrzeugdynamische Systemanalyse**, *Eisenbahningenieur*, 53 (2002), No. 7, pp. 50-57
19. LOGSTON, C F, JR. & ITAMI, G S: **Locomotive friction-creep studies**, *ASME Journal of Engineering for Industry*, 102 (1980), pp. 275-281
20. ENGEL, B, BECK, H P & ALDERS, J: **Verschleißreduzierende Radschlupfregelung mit hoher Kraftschlussausnutzung**, *Elektrische Bahnen*, 96 (1998), No. 6, pp. 201-209
21. LANG, W & ROTH, G: **Optimale Kraftschlussausnutzung bei Hochleistungs-Schienefahrzeugen**, *Eisenbahntechnische Rundschau*, 42 (1993), No. 1-2, pp. 61-66
22. POLACH, O: **Influence of locomotive tractive effort on the forces between wheel and rail**, *Selected papers from the 20th International Congress of Theoretical and Applied Mechanics held in Chicago, 28 August - 1 September 2000, Vehicle System Dynamics Supplement*, 35 (2001), pp. 7-22
23. KOSSMANN, C: **Design calculation and verification using SIMPACK Wheel/Rail at Bombardier Transportation Winterthur**, SIMPACK User Meeting, 13.-14. 11. 2001, Bad Ischl, Austria, In Internet: [www.simpack.de](http://www.simpack.de)